SUPPLEMENTARY INFORMATION

Engineering of a 3D-Printed Hierarchically Channeled Solar Reactor for Thermochemical Fuel Production

Sebastian Sas Brunser, Eike Lage, Dario Walde, and Aldo Steinfeld*
Department of Mechanical and Process Engineering, ETH Zurich, 8092 Zurich, Switzerland

1. High Flux Solar Simulator (HFSS)

The solar radiative power P_{solar} and its flux distribution delivered by the ETH's High Flux Solar Simulator (HFSS) that is incident at the solar reactor's aperture were measured using a calibrated CCD camera focused on a Lambertian target and a water calorimeter. The water calorimeter incorporated the identical front flange and quartz window as the solar reactor, eliminating the need for transmissivity corrections. These measurements were critical to accurately determine $\eta_{solar-to-fuel}$. Fig. S1 shows the measured data for the two HFSS configurations. The total error in the measured value of P_{solar} was $\pm$4.7%.

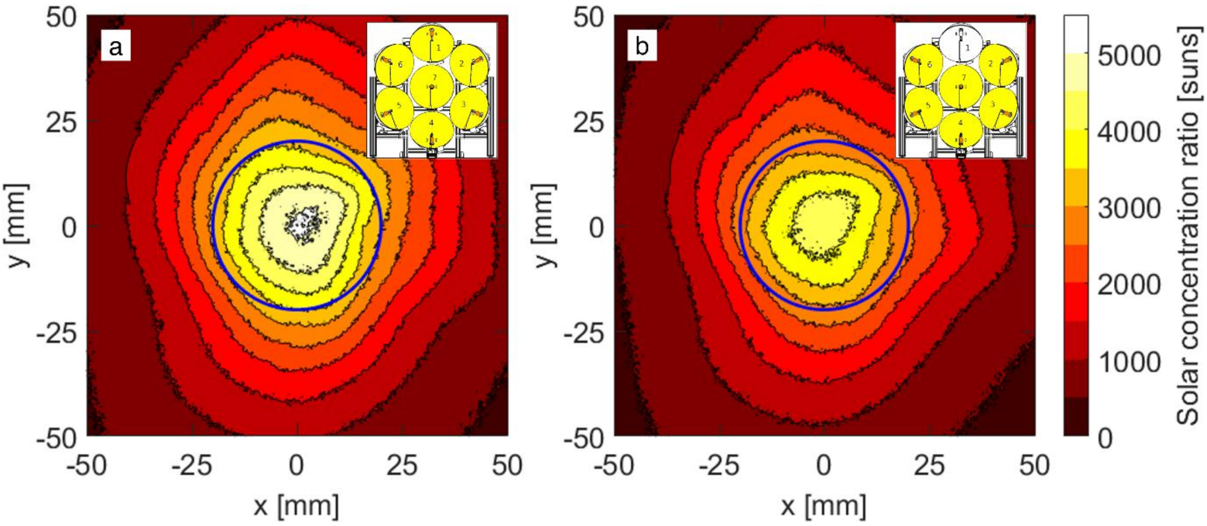

Figure S1: Measured radiative flux maps for two HFSS arc configurations (see insets) applied in the experimental runs. The solar reactor's 40 mm-diameter circular aperture is indicated by the blue circle. Peak/average flux concentrations: a) 5100/4082 suns; b) 4200/3454 suns. The solar radiative power input P_{solar}: a) 5.13±0.24 kW; b) 4.34±0.20 kW.

* Corresponding author. E-mail address: aldo.steinfeld@ethz.ch (A. Steinfeld).

2. Thermocouple placement in the solar reactor

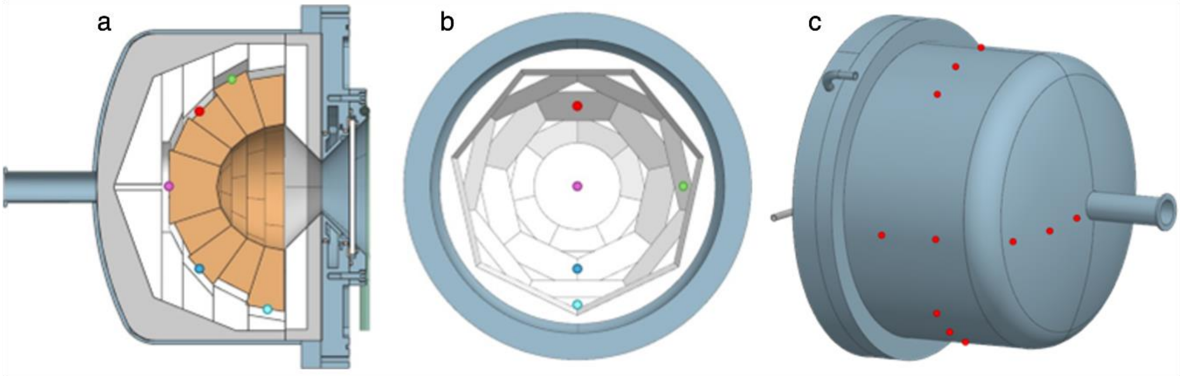

Figure S2: (a) Cross section and (b) front view of the solar reactor showing the placement of the five B/S-type thermocouples. The thermocouples are inserted touching the back of the ceria bricks. (c) Placement of the 11 K-type thermocouples measuring the temperature of the stainless-steel shell.

3. Modified lighter thermal insulation

The five rings composing the rear section of the Zirconia ZYZ-3 thermal insulation were drilled to remove 261 g, about 21% of the original weight (see Fig. S3).

Figure S3: Photographs of the five rings comprising the back ZYZ-3 insulation part after drilling.

4. Solar-to-Fuel Energy Efficiency

The formulation is extracted from Ref. [1]. The solar-to-fuel energy efficiency $\eta_{\text{solar-to-fuel}}$ is defined as the ratio of the heating value of the syngas produced to the sum of Q_{solar} and any other parasitic energy inputs such as those associated with vacuum pumping and/or inert gas consumption during the reduction step:

$$\eta_{\text{solar-to-fule}} = \frac{Q_{\text{fuel}}}{Q_{\text{input}}} = \frac{Q_{\text{fuel}}}{Q_{\text{solar}} + Q_{\text{pump}} + Q_{\text{inert}}} \tag{1}$$

Q_{fuel} is the heating value of the fuel (CO and H_2) produced over a cycle, given by:

$$Q_{\text{fuel}} = \sum_{\text{fuel: } H_2,\text{CO}} \Delta H_{\text{fuel}} \int r_{\text{fuel}} dt \tag{2}$$

where ΔH_{fuel} is the molar enthalpy change of fuel oxidation (e.g. ΔH_{CO} =283 kJ/mol, ΔH_{H_2} = 286 kJ/mol) and $\int r_{\text{fuel}} dt$ is the measured molar rate of the fuel produced integrated over the duration of the oxidation step. Q_{solar} is the total solar energy input integrated over the duration of the cycle:

$$Q_{\text{solar}} = \int P_{\text{solar}} dt \tag{3}$$

where P_{solar} is the measured solar radiative power input through the solar reactor. Q_{pump} and Q_{inert} are the thermal energy penalties associated with vacuum pumping and inert gas consumption during the reduction step. All work terms are converted to an equivalent heat by dividing by a heat-to-work efficiency $\eta_{heat\text{-}to\text{-}work}$ (assumed 0.4). In this way, the entire thermochemical process chain is driven using solar heat alone. Q_{pump} is calculated as the thermodynamic minimum pumping work divided by the product of two efficiencies, namely the heat-to-work efficiency $\eta_{heat\text{-}to\text{-}work}$ and the vacuum pump efficiency η_{pump}, according to:

$$Q_{\text{pump}} = \frac{1}{\eta_{\text{heat-to-work}} \cdot \eta_{\text{pump}}} \int \dot{n}(t) \cdot R \cdot T \cdot \ln\left(\frac{p_{\text{atmospheric}}}{p_{\text{cavity}}(t)}\right) dt \quad (4)$$

where $\dot{n}(t)$ is the sum of the measured molar flow rates of Ar injected and O_2 released by ceria during the reduction step, p_{cavity} is the measured total pressure inside the cavity and $p_{atmospheric}$ is the atmospheric pressure. The pump efficiency for a multi-stage industrial arrangement is given by:

$$\eta_{\text{pump}} = 0.07 \cdot \log\left(\frac{p_{\text{cavity}}}{p_{\text{atmospheric}}}\right) + 0.4 \quad (5)$$

Note that $\eta_{solar\text{-}to\text{-}syngas}$ is weakly depended on η_{pump} because $Q_{solar} >> Q_{pump}$ at the moderate vacuum pressure levels applied during reduction in the range 10-1000 mbar. The thermal energy required for inert gas separation is given by:

$$Q_{\text{inert}} = \frac{1}{\eta_{\text{heat-to-work}}} E_{\text{inert}} \int r_{\text{inert}} dt \quad (6)$$

where r_{inert} is the measured Ar flow rate and E_{inert} is the work required for inert gas separation, assumed 20 kJ per mole.

5. Measured performance for 68 redox cycles

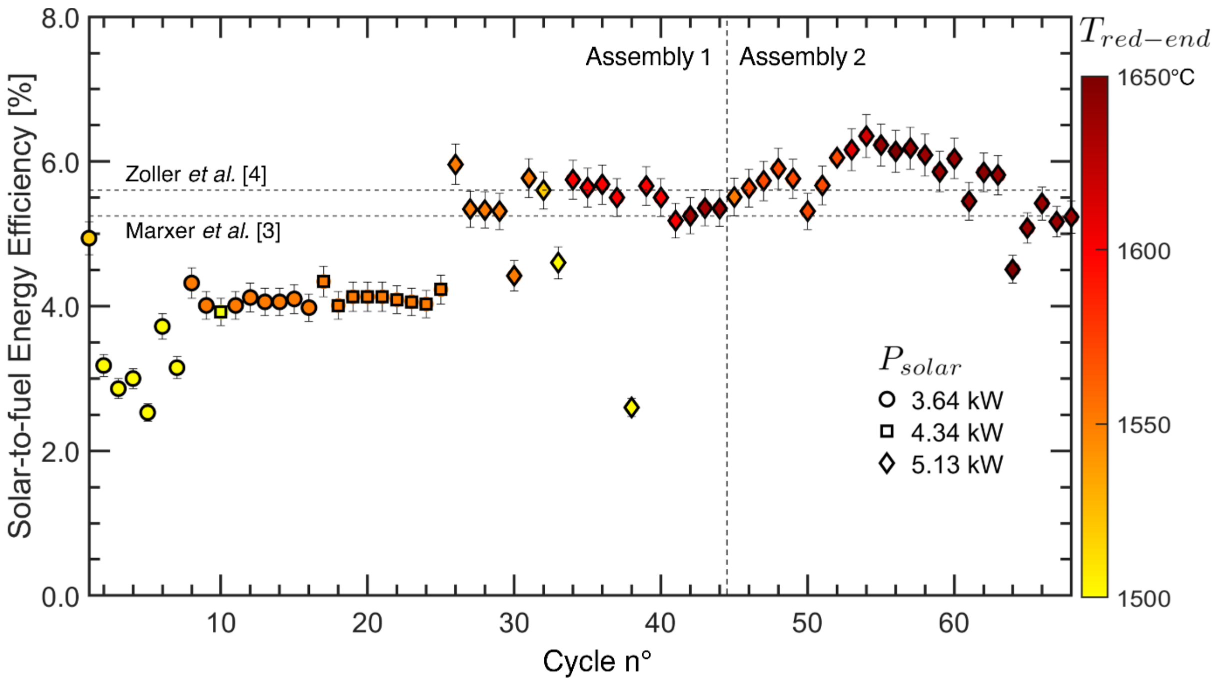

Figure S4: Solar-to-fuel energy efficiencies $\eta_{solar-to-fuel}$ with error bars for 68 redox cycles performed during two experimental campaigns using the solar reactor with two thermal insulation assemblies: 44 and 24 consecutive cycles with assembly 1 and 2, respectively. Assembly 1: solar reactor with original thermal insulation. Assembly 2: solar reactor with modified (lighter) thermal insulation. Colors indicate values for $T_{\text{reduction-end}}$; shapes indicate values for P_{solar}. Horizontal dashed lines indicate the previous measured values of $\eta_{solar-to-fuel}$ obtained in Refs. [2] and [3], added for comparison.

6. References

1. Schappi, R., Rutz, D., Dahler, F., Muroyama, A., Haueter, P., Lilliestam, J., Patt, A., Furler, P., & Steinfeld, A., *Drop-in fuels from sunlight and air.* Nature, 2022. **601**(7891): p. 63-68.DOI: 10.1038/s41586-021-04174-y.
2. Marxer, D., Furler, P., Takacs, M., & Steinfeld, A., *Solar thermochemical splitting of CO_2 into separate streams of CO and O_2 with high selectivity, stability, conversion, and efficiency.* Energy & Environmental Science, 2017. **10**(5): p. 1142-1149.DOI: 10.1039/c6ee03776c.
3. Zoller, S., Koepf, E., Nizamian, D., Stephan, M., Patané, A., Haueter, P., Romero, M., Gonzalez-Aguilar, J., Lieftink, D., de Wit, E., Brendelberger, S., A., S., & Steinfeld, A., *A solar tower fuel plant for the thermochemical production of kerosene from H_2O and CO_2.* Joule, 2022. **6**: p. 1-11.DOI: 10.1016/j.joule.2022.06.012.